Korean J. Chem. Eng., 33(4), 1337-1344 (2016)
DOI: 10.1007/s11814-015-0279-4

pISSN: 0256-1115
eISSN: 1975-7220

Preparation of γ-alumina nanoparticle modified polyacrylamide composite and study on its solid phase extraction of Sunset Yellow

Wanjun Li*,†, Qiong Jia, Zhenyu Zhang***, and Yuanpeng Wang****

*Department of Chemistry and Chemical Engineering, Taiyuan Institute of Technology, Taiyuan 030008, P. R. China
**College of Chemistry, Jilin University, Changchun 130012, P. R. China
***State Key Laboratory of Supramolecular Structure and Materials, College of Chemistry, Jilin University, Changchun 130012, P. R. China
(*Received 26 August 2015 • accepted 11 December 2015*)

Abstract−An organic-inorganic composite, γ-alumina nanoparticle modified polyacrylamide, was synthesized in this study. The composite was characterized by scanning electron microscope, nitrogen adsorption-desorption measurement, thermal gravimetric analyzer, differential scanning calorimetry, and Fourier-transformed infrared spectrometer. A novel solid-phase extraction method with the synthesized composite as the adsorbent was developed for the enrichment of Sunset Yellow coupled with ultraviolet-visible spectrophotometry. To obtain the optimum extraction efficiency, the experimental parameters in the processes of preparation of the adsorbent and solid-phase extraction were studied including synthesis temperature, synthesis time, the dosage of γ-alumina nanoparticles, sample flow rate, sample pH, eluant concentration, and eluant flow rate. Under the optimum conditions, the detection limit of the developed method was calculated to be 0.037 μg mL^{-1} with intra-day and inter-day relative standard deviation values of 2.57% and 3.89%, respectively. When the method was applied to the determination of Sunset Yellow in beverages, satisfactory recoveries were obtained in the range of 92.3-109.8%.

Keywords: γ-Alumina Nanoparticle, Polyacrylamide, Solid-phase Extraction, Sunset Yellow, Spectrophotometry

INTRODUCTION

Synthetic dyes are an important kind of food additive, which are widely used to provide the desired colored appearance of food, and compensate for the loss of natural colors [1]. However, most synthetic dyes are aniline compounds made of benzene, toluene, and naphthalene. Some of these substances pose potential harm to human organism, especially if they are excessively consumed [2]. The addition of synthetic dyes in food is strictly controlled by legislation across many countries [3]. Therefore, the detection of their concentrations is of prime importance.

Various analytical techniques have been introduced to measure concentrations of synthetic dyes including high performance liquid chromatography (HPLC) [4], ultra-fast liquid chromatography-tandem mass spectrometry (UFLC-MS/MS) [5], electroanalytical methods [6], and spectrophotometry [7,8]. However, taking into account the complex matrix effect and low level concentrations of synthetic dyes in food samples, direct determination of them is often difficult. Thus, the enrichment and pretreatment step is necessary before the detection of synthetic dyes to enhance the sensitivity and selectivity [9].

Many kinds of methods have been developed for preconcentration of synthetic dyes, such as liquid-liquid extraction (LLE) [10], cloud point extraction (CPE) [11], solid-phase microextraction (SPME) [12,13], and solid-phase extraction (SPE) [14,15]. However, the drawbacks of LLE and CPE are well known of being time-consuming, complexity, and high consumption of toxic organic solvents [16]. SPME offers the advantage of less use of toxic solvents than LLE and CPE. Nevertheless, SPME fiber has a limited lifetime which is always fragile, and its sample carry-over also has problems. SPE is one of the most effective and widely applicable approaches owing to its simple operation, easy separation, high efficiency, and low consumption of toxic organic solvents [17,18].

The adsorbents of the SPE technique are very important as extraction medium. Various materials were selected as adsorbents for synthetic dyes including activated carbon [19,20], solid waste [21,22], zeolite [23], and organic polymer [24,25]. Activated carbon and solid waste are widely used for the adsorption of many kinds of organics, but their intrinsic limitation is that these materials are difficult to recycle, and have been widely diffused into the environment to become a secondary source of environmental pollution [26]. In these materials, organic polymer has also been widely used because of fast mass transfer kinetics, high loading capacity, regeneration ability and reuse for continuous processes [27,28]. However, they also suffer from swelling and shrinkage when exposed to different organic solvents, leading to weak mechanical stability [29,30]. In recent years, new materials, which have specific chemical properties depending on the modification of polymers with inorganic materials, have been designed, featuring high surface-to-volume ratio, specific chemical properties, strong mechanical stability, and high regenerability [31-33].

γ-Alumina nanoparticles are a kind of inorganic material with

†To whom correspondence should be addressed.
E-mail: lwjchemistrytit@sina.com

significant potential in sorptive extraction owing to their uniform particle size, high surface area, strong ability of adsorption, and excellent dispersibility in many solvents [34,35]. Hydroxyl groups on the surface of γ-alumina nanoparticles can interact with specific functional groups, which may improve the adsorption performance [34]. The aim of the present work was to develop a simple and sensitive SPE method for the preconcentration of Sunset Yellow coupled with spectrophotometric detections. In the method, the adsorbent of γ-alumina nanoparticle modified polyacrylamide composite (hereafter abbreviated as ANMPC) was used as the extraction medium, which was prepared by one-step synthesis procedure. As far as we know, it is the first time that an SPE method with ANMPC as the adsorbent is applied to the determination of Sunset Yellow in beverage samples.

EXPERIMENTAL

1. Chemicals and Solutions

Acrylamide (AAm) was purchased from Tianjin Guangfu Fine Chemical Research Institute (Tianjin, China). *N*, *N*′-methylene bisacrylamide (MBAAm) was obtained from Sigma-Aldrich (USA). γ-Alumina nanoparticles were purchased from Aladdin Reagent (Shanghai, China). Dodecanol, dimethylsulfoxide (DMSO), acetone, methanol, ethanol, and azobisisobutyronitrile (AIBN) were obtained from Tianjin Chemical Plant (Tianjin, China). AAm and AIBN were purified by recrystallization from acetone and ethanol, respectively, followed by drying in vacuum at room temperature. Sunset Yellow was purchased from TCI (Tokyo, Japan). The structure of Sunset Yellow is shown in Fig. 1.

The stock standard solution of 1,000 μg mL^{-1} of the target analyte was prepared in deionized water. The stock standard solution and diluted standard solutions were stored in brown glass volumetric flasks at 4 °C. All solvents and sample solutions for the spectrophotometric analysis were filtered through a Millipore filter (pore size 0.45 μm). Deionized water was used for all the experiments.

2. Instrument and Analytical Conditions

A KQ-50DB digital ultrasonic cleaner (Jiangsu Kunshan Ultrasonic Instruments Co., Ltd., China) was used for removing oxygen of the pre-polymerization mixture solution and getting a homogeneous solution. An LSP01-1A programmable syringe pump (Baoding Longer Precision Pump Co., Ltd., Hebei, China) was used for pushing solutions. For pH measurements, a pHS-3C digital pH meter (Shanghai Rex Instruments Factory, China) was employed.

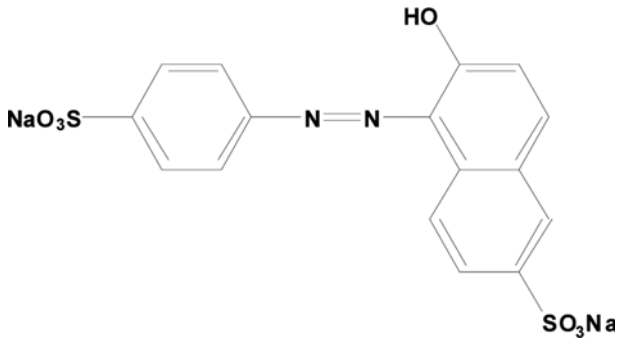

Fig. 1. The molecular structure of Sunset Yellow.

A TU 1201 ultraviolet-visible (UV-Vis) spectrophotometer (Beijing Purkinje General Instruments Co., Ltd., China) was used for the spectrophotometric analysis. The UV-Vis absorbance detection was set to 482 nm. The microscopic morphology of the adsorbent was observed by a scanning electron microscope (SEM, JEOL JSM-6700F, Japan). Nitrogen adsorption-desorption analysis was performed on an Autosorb Station1 instrument (Quantachrome, USA). The material was evacuated under vacuum and heated to 120 °C for 10 h before analysis. The Brunauer-Emmett-Teller (BET) surface area was calculated from adsorption data at a relative pressure ranging from 0.066 to 0.30. Mesopore size distributions were evaluated from adsorption branches using the Barrett-Joyner-Halenda (BJH) model. The thermal properties of the polyacrylamide material and ANMPC were investigated by thermal gravimetric analysis (TGA) and differential scanning calorimetry (DSC). TGA and DSC measurements were performed on a TA Q500 thermogravimeter (TA, USA) and NETZSCH DSC204 instrument (NETZSCH, German), respectively, at the heating rate of 10 °C min^{-1} under nitrogen. Fourier-transformed infrared (FT-IR) spectra were obtained by using a SPECTRUN-100 FT-IR instrument (PerkinElmer, USA).

3. Synthesis of ANMPC

In preliminary experiments, γ-alumina nanoparticles were proven to be dispersed homogeneously in binary porogens, DMSO and dodecanol. The pre-polymerization solution which contained 70.0 mg AAm, 130.0 mg MBAAm, 2.0 mg AIBN, mixture of DMSO (682.0 mg), dodecanol (357.0 mg) and γ-alumina nanoparticles (60.0 mg) was sonicated for 10 min to remove oxygen and obtain a uniform solution. The reaction was initiated at 60 °C for 5 h to synthesize ANMPC. After the completeness of the reaction, ANMPC was washed with DMSO, methanol, deionized water, and methanol in turn to remove porogens and unreacted components. Finally, ANMPC was dried in an oven at 60 °C for 2 h.

4. Sample Preparation

Different brands of nine beverage samples (three fruit juices, three carbonated beverages, and three pre-mix cocktails) were purchased from local supermarkets and stored in a refrigerator. Optimization studies of experimental parameters in the processes of both ANMPC preparation and SPE were carried out with a blank sample which did not contain Sunset Yellow. Each sample was degassed in the ultrasonic bath for 20 min. 1 mL sample was diluted with phosphate buffered solution (PBS) (0.02 mol L^{-1}, pH=2.0) in a brown volumetric flask. The sample solutions were filtered through a Millipore filter (pore size 0.45 μm) and the filtrate was stored in brown volumetric flasks of 10 mL at 4 °C for the SPE steps.

5. SPE Process

Before SPE, 20 mL 5% H_2SO_4 solution, 30 mL deionized water, and 20 mL ethanol were passed through the microcolumn in sequence at a flow rate of 2.0 mL min^{-1} to clean the impurities [36]. 0.2 g ANMPC was packed into the microcolumn. The SPE process consisted of four successive steps (preconditioning, sample loading, washing, and desorption). For preconditioning, 0.4 mL methanol was pushed to pass through the microcolumn at a flow rate of 0.5 mL min^{-1}, and then 2.0 mL NaH_2PO_4 (pH=2.0) was

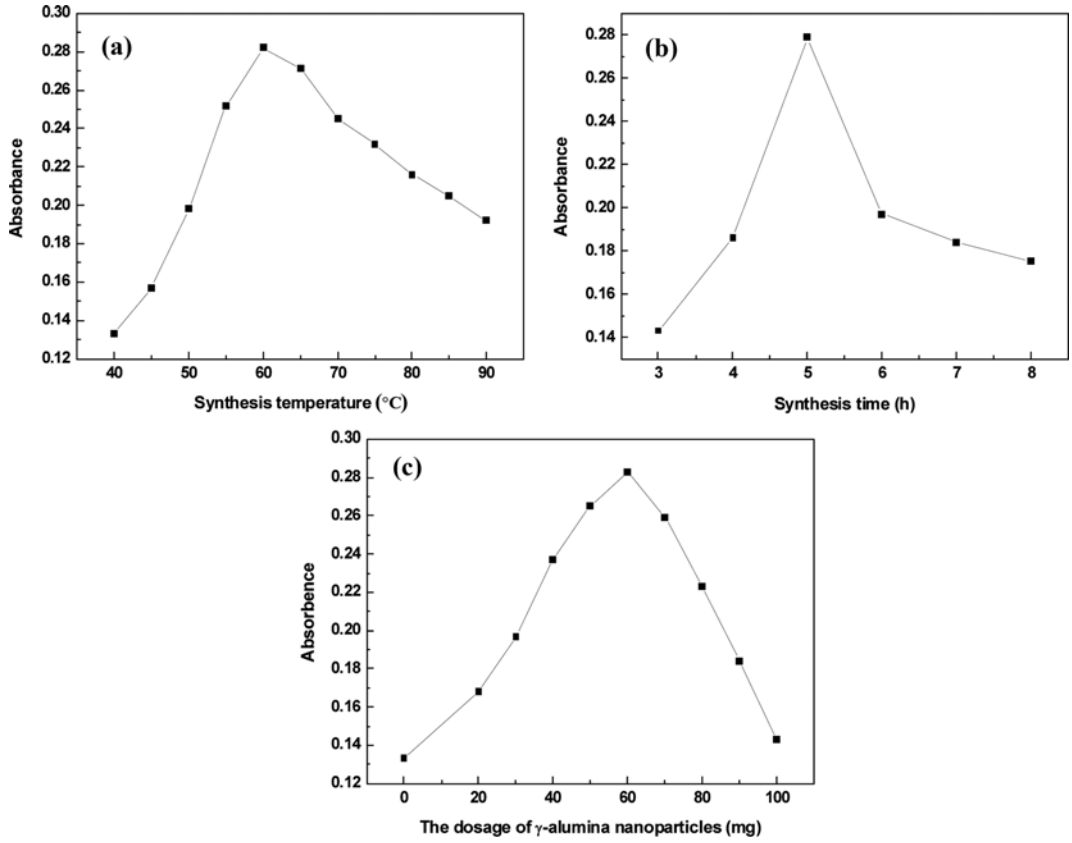

Fig. 2. Optimization of synthesis temperature (a), synthesis time (b), and the dosage of γ-alumina nanoparticles (c) for preparation of the adsorbent. Sunset Yellow concentration: 2 μg mL^{-1}. The extraction and spectrophotometry conditions are outlined in "EXPERIMENTAL".

expelled at 1.5 mL min^{-1}. After that, 4.0 mL sample solution was loaded onto the microcolumn at a flow rate of 1.0 mL min^{-1}. In the washing step, 1.0 mL NaH_2PO_4 (pH=2.0) was expelled to flow through the microcolumn at a flow rate of 1.5 mL min^{-1} to wash impurities of samples which were not adsorbed by ANMPC. In the desorption step, 1.0 mL eluant, *i.e.*, 2.0% ammonia solution/methanol (2 : 1, *V/V*), was injected to the microcolumn at a flow rate of 0.5 mL min^{-1} and the eluate was collected for UV-Vis detections.

RESULTS AND DISCUSSION

1. Preparation of ANMPC

We selected two monomers, AAm and MBAAm, to synthesize ANMPC. DMSO and dodecanol were chosen as porogens and the weight ratio of monomers/porogens was approximately 1/5 [4]. Polyacrylamide-based materials have specific adsorption capacity of synthetic dyes which contain phenolic groups and/or sulfo groups [37]. And the adsorption capacity is caused by the hydrogen bonding interaction between the amide group of polyacrylamide and the sulfo group and/or the phenolic group of Sunset Yellow. The procedure for preparation of ANMPC is presented in "EXPERIMENTAL." To access the best extraction efficiency of the SPE method, several experimental parameters in the synthesis procedure including synthesis temperature, synthesis time, and the dosage of γ-alumina nanoparticles, were investigated.

As is well known, polyacrylamide materials can offer three-dimensional porous structures [4]. The porous structure of the composite, especially the pore size which depends on the synthesis temperature, affects the extraction efficiency. Therefore, we investigated the influence of synthesis temperature on the extraction efficiency from 40 to 90 °C. As shown in Fig. 2(a), the absorbance first increased, but then decreased after reaching a maximum value at the synthesis temperature of 60 °C. We also did BET analysis for the composites prepared at different synthesis temperatures (40, 60, and 80 °C), indicating that the pore sizes were 37.4, 30.7, and 26.4 nm with BET surface areas of 77.2, 90.7, and 97.8 m^2 g^{-1}, respectively. These results were in accordance with Xie et al's work [38], *i.e.*, higher synthesis temperature led to smaller pores and higher BET surface area as a result of higher synthesis rate. When the synthesis temperature was too low, too large pores led to too low surface areas of the composites, which decreased the extraction efficiency of the composite. However, when the synthesis temperature was too high, too small pores caused too high back pressure of the composite, which would be unfavorable to the extraction. As a consequence, 60 °C was chosen as the synthesis temperature.

To examine the effect of synthesis time on the extraction efficiency, we looked at synthesis time within the range of 3-8 h. As shown in Fig. 2(b), the absorbance increased in the beginning and decreased when the synthesis time was longer than 5 h. BET analysis was also carried out for the composites prepared at different synthesis time (4, 5, and 6 h), demonstrating that the pore sizes were 32.5, 30.7, and 29.4 nm with BET surface areas of 87.4, 90.7,

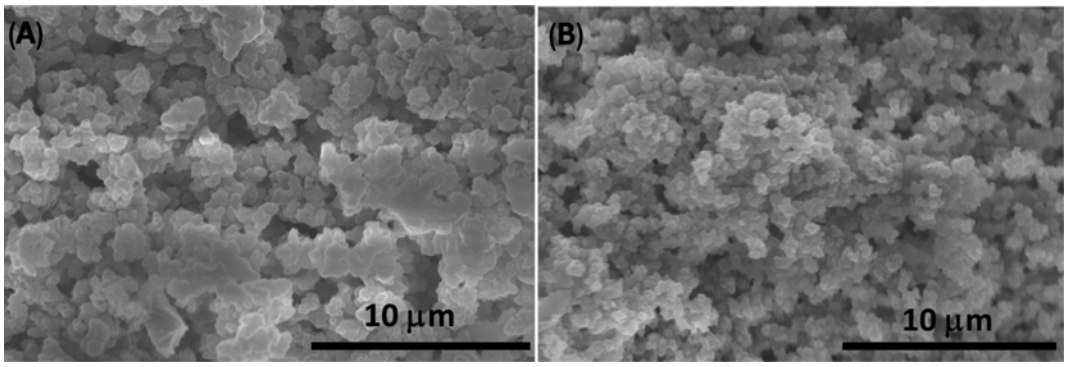

Fig. 3. SEM micrographs of the polyacrylamide material (A) and ANMPC (B).

and 92.6 m^2 g^{-1}, respectively. The same results, *i.e.*, longer synthesis time led to smaller pores and higher BET surface areas because of higher conversion of the reaction, were reported by Svec et al. [39]. When the synthesis time was too short, too large pores led to too low surface area of the composite, which decreased the extraction efficiency of the composite. Nevertheless, when the synthesis time was too long, too small pores led to too high back pressure of the composite and too low extraction efficiency. Therefore, 5 h was selected as the optimized synthesis time.

The effect of the dosage of γ-alumina nanoparticles on the extraction efficiency was investigated in the range of 0-90 mg. Fig. 2(c) shows that the composite manifested better enrichment ability than the unmodified polyacrylamide, indicating that γ-alumina nanoparticles participated in the adsorption of Sunset Yellow. The adsorption was attributed to the hydrogen bonding interaction between the hydroxyl group of the γ-alumina nanoparticle and the sulfo group and/or the phenolic group of Sunset Yellow. Moreover, the composite mixed with 60 mg γ-alumina nanoparticles had the highest extraction efficiency. BET experiments were also carried out for the composites prepared with different dosages of γ-alumina nanoparticles (0, 60, and 90 mg), indicating that the pore sizes were 311.5, 30.7, and 18.2 nm with BET surface areas of 31.6, 90.7, and 120.4 m^2 g^{-1}, respectively. It could be concluded that the pore size of the composite decreased and the BET surface area increased with increasing the dosage of γ-alumina nanoparticles. When the dosage of γ-alumina nanoparticles was too large, too small pores led to too high back pressure of ANMPC and too low extraction efficiency. However, when the dosage of γ-alumina nanoparticles was less, the hydrogen bonding interactions decreased and the swelling of the composite increased, which decreased the extraction efficiency of the composite. Considering the extraction efficiency, we selected 60 mg as the dosage of γ-alumina nanoparticles.

2. Characterization of ANMPC

The morphologies of the polyacrylamide material and ANMPC are shown in Fig. 3. The SEM micrograph is shown in Fig. 3(B), illustrating that the structure of ANMPC is a homogeneous network of the macroporous polymer which was highly cross-linked. The micrographs clearly demonstrated that the size of the microglobules and the pores in ANMPC was smaller than that in the polyacrylamide material, demonstrating that the polyacrylamide microglobules might be modified with γ-alumina nanoparticles.

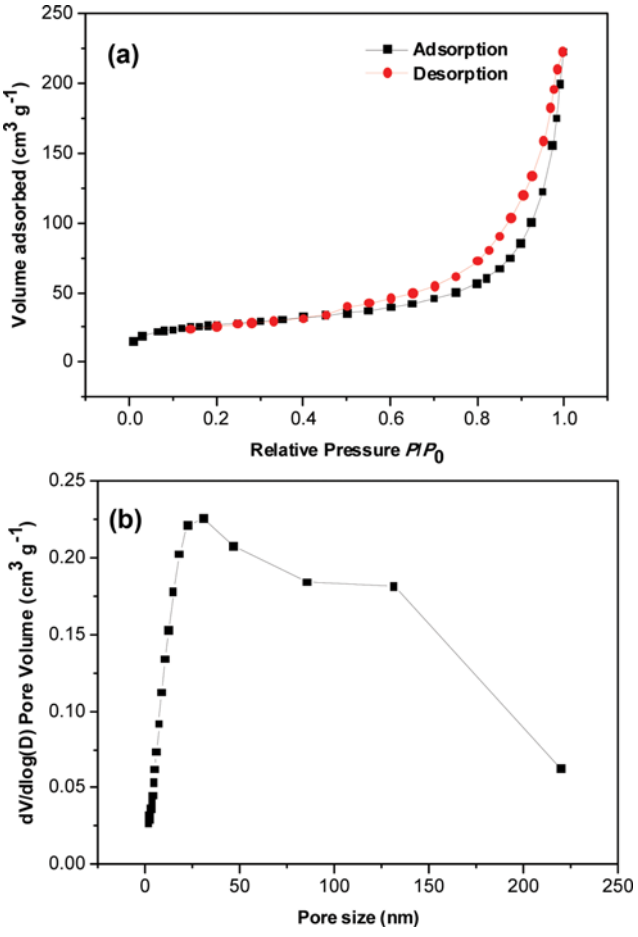

Fig. 4. Nitrogen adsorption-desorption isotherm (a) and pore size distribution (b) of ANMPC.

The nitrogen adsorption-desorption isotherm of ANMPC showed typical type IV curves (Fig. 4(a)), suggesting the presence of mesopores. As mentioned in "Preparation of ANMPC," the pore size of ANMPC was 30.7 nm, which was calculated from the adsorption data using the BJH model (Fig. 4(b)). The calculated BET surface area was 90.7 m^2 g^{-1}, while that of the polyacrylamide material was 31.6 m^2 g^{-1}, implying that the embedded γ-alumina nanoparticles effectively increased the surface area of ANMPC.

The thermal properties of the polyacrylamide material and

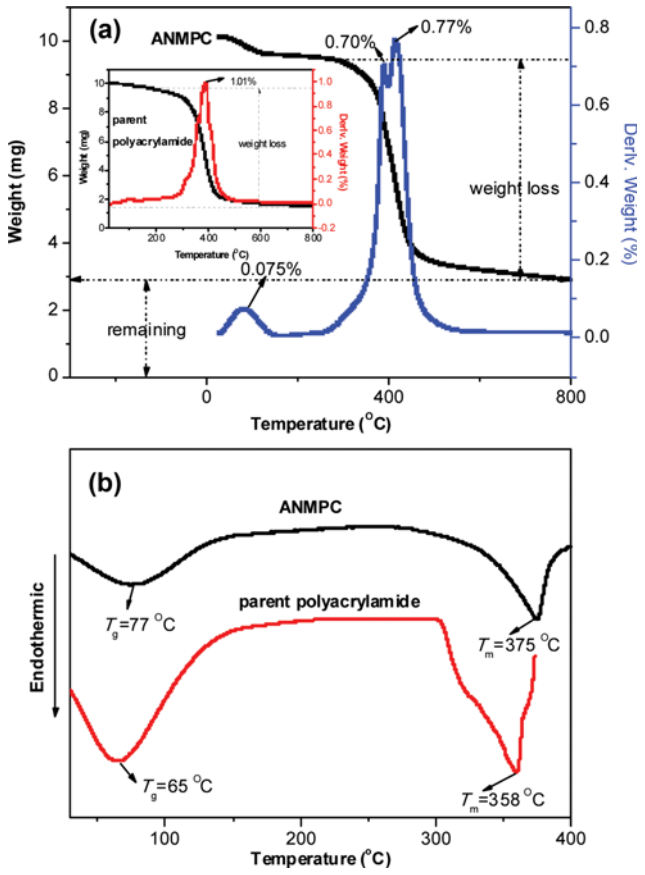

Fig. 5. TGA (a) and DSC (b) curves of the polyacrylamide material and ANMPC.

ANMPC were investigated by TGA and DSC under nitrogen atmosphere at the heating rate of 10 °C min^{-1}. As shown in Fig. 5(a), the weight loss of the polyacrylamide material appeared in the range of 260-490 °C, while that of ANMPC appeared from 295 to 535 °C. Moreover, the residual mass of ANMPC after the weight loss was much greater than that of the polyacrylamide in the same temperature range. Fig. 5(b) depicts the DSC curves of the two materials. The powder sample of the polyacrylamide material showed two intense endothermic peaks at 65 °C and 358 °C during the heating process, corresponding to its glass transition temperatures (T_g) and melting points (T_m). Similarly, the T_g and T_m of ANMPC were 77 °C and 375 °C, respectively, which were higher than that of the polyacrylamide material. Overall, the embedded γ-alumina nanoparticles could greatly improve the thermal stability of the material.

To investigate the combining way of γ-alumina nanoparticle and polyacrylamide in ANMPC, we studied the FT-IR spectra of γ-alumina nanoparticles (Fig. 6(a)), the polyacrylamide material (Fig. 6(b)), and ANMPC (Fig. 6(c)). According to the FT-IR spectra of γ-alumina nanoparticles, the characteristic peak was at 3,458 cm^{-1} for -OH, and there was a wide absorption band at 400-1,000 cm^{-1} [40]. According to the FT-IR spectra of the polyacrylamide material, the characteristic peaks were at 3,332 cm^{-1} and 1,647 cm^{-1} for -N-H stretching vibrations and -C=O of amide groups. As shown in Fig. 6(c), the characteristic peaks of ANMPC were at 3,371 cm^{-1} and 1,656 cm^{-1} for -N-H stretching vibrations and -C=O of amide

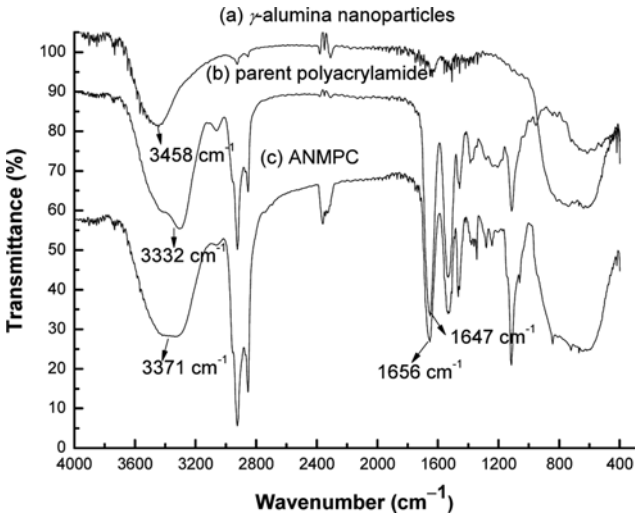

Fig. 6. FT-IR spectra of γ-alumina nanoparticles (a), the polyacrylamide material (b), and ANMPC (c).

groups, and a wide absorption band was at 400-1,000 cm^{-1}. However, no other characteristic peaks appeared in the FT-IR spectra of ANMPC. It could be concluded that γ-alumina nanoparticles and polyacrylamide combined by a way of physical adsorption.

3. Effects of Experimental Conditions on the SPE Process

To obtain the best extraction efficiency, several experimental conditions including sample flow rate, sample pH, eluant concentration, and eluant flow rate were investigated when the concentration of Sunset Yellow was 2 μg mL^{-1}. The absorbance of the target analyte as the UV-Vis spectrophotometric response was used to evaluate the extraction efficiency under various experimental conditions.

The sample flow rate has great influence on the sorption of the target analyte on the microcolumn containing the adsorbent. As shown in Fig. 7(a), the absorbance first increased but then decreased after reaching a maximum value. As is well known, a low sample flow rate is not employed to avert long extraction time, which leads to a decrease of determination efficiency and wide absorption peaks. However, too high sample flow rate results in the incomplete adsorption of the target analyte, because the sample solution passes through the microcolumn too fast, which results in low extraction efficiency. As a result, the sample flow rate of 1.0 mL min^{-1} was selected for the following experiments.

Sample pH is an important parameter influencing the quantitative adsorption and recovery of the target analyte. It always affects the interactions between the adsorbent and the target analyte. The effect on the absorbance was investigated when the sample pH values were adjusted from 1.0 to 10.0 with H_3PO_4 or NaOH solutions. As shown in Fig. 7(b), the absorbance first increased and then decreased after reaching a maximum value. This may be explained by the interactions between ANMPC and Sunset Yellow, which originated from electrostatic repulsion and hydrogen bonding. There are two kinds of hydrogen bonding in this system. One is formed by the interaction between the amide group of polyacrylamide and the sulfo group and/or the phenolic group of Sunset Yellow. The other is attributed to the interaction between

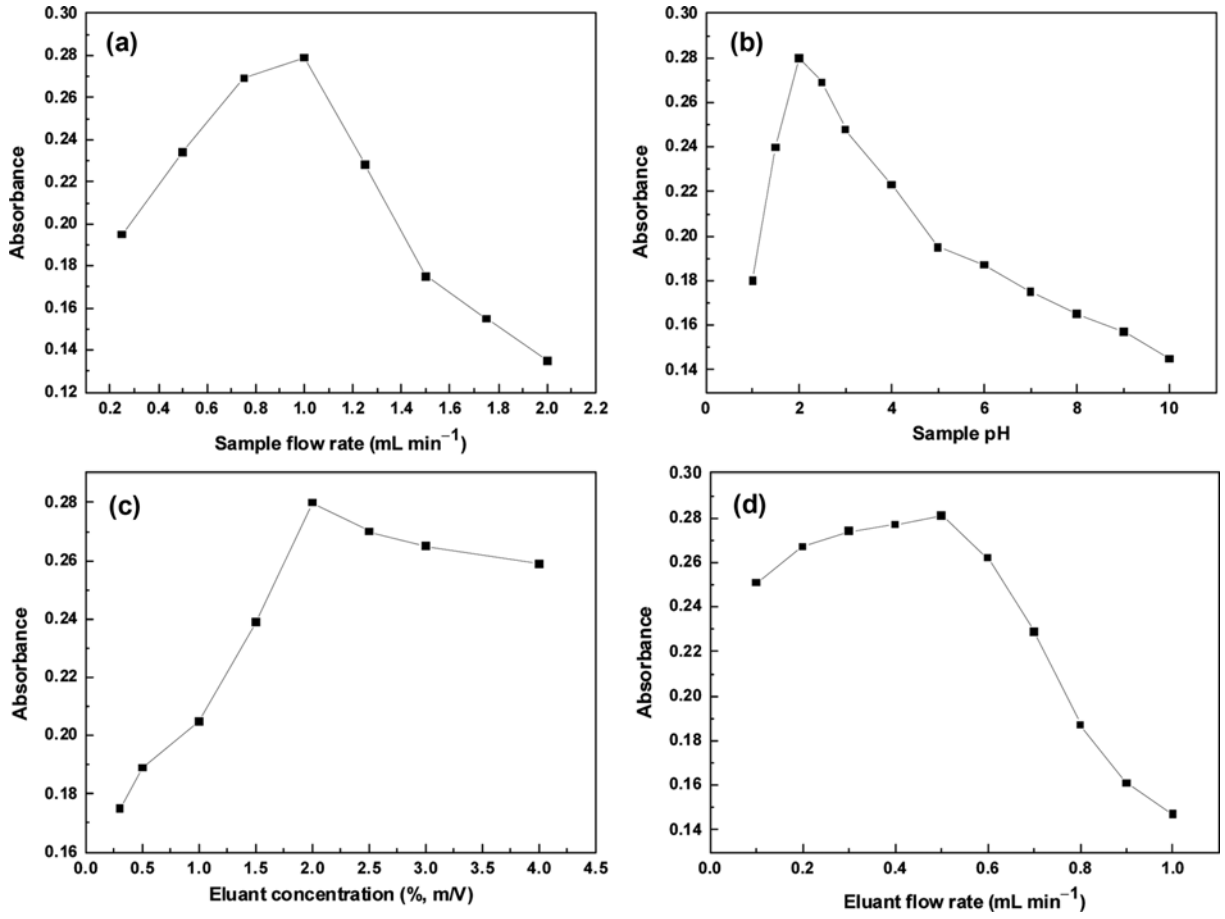

Fig. 7. Effects of experimental conditions on the SPE for 2 μg mL^{-1} Sunset Yellow, including sample flow rate (a), sample pH (b), eluant concentration (c), and eluant flow rate (d). The extraction and spectrophotometry conditions are outlined in "EXPERIMENTAL."

the sulfo group and/or the phenolic group of Sunset Yellow and the hydroxyl group of the γ-alumina nanoparticle, which is formed when the γ-alumina nanoparticles are exposed to protic solvents [4,37]. When pH is too low, the electrostatic repulsion increases due to the protonation of Sunset Yellow and ANMPC. The decrease of the absorbance at high pH is due to the decrease of the hydrogen bonding interaction. As a result, sample pH of 2.0 was chosen in the present work.

To guarantee an effective elution of the absorbed analyte on the microcolumn, the effect of eluant concentration (the concentration of ammonia in eluant) on the extraction efficiency was investigated in the range of 0.3-4.0%. As shown in Fig. 7(c), the absorbance of Sunset Yellow first increased with the increasing concentration and decreased at higher concentrations, and the maximum absorbance was at the concentration of 2.0%. Hence, the eluant concentration of 2.0% was chosen for desorption of Sunset Yellow. In addition, the effect of the eluant flow rate was studied in the range of 0.1-1.0 mL min^{-1}. Fig. 7(d) indicates that the absorbance of Sunset Yellow first increased and then decreased at higher flow rate. Finally, the eluant flow rate of 0.5 mL min^{-1} was selected for the experiments.

4. Analytical Feature and Method Validation

Under the optimum experimental conditions, several experiments were carried out to assess the proposed SPE method. The correlation coefficient (r) was achieved as 0.9971 with the Sunset Yellow concentration range of 0.250 μg mL^{-1}. Other performances of the SPE method with ANMPC were also investigated. The limit of detection (LOD) and limit of quantification (LOQ) values, determined as *S*/*N* ratios of 3 and 10, were 0.037 μg mL^{-1} and 0.12 μg mL^{-1}, respectively. The intra-day and inter-day relative standard deviations (RSDs) were obtained as 2.57% and 3.89% (n=7), respectively. The enrichment factor value by the ratio of the slopes of calibration curves with/without employing the SPE method was calculated as 17.1. Hence, the method had good sensitivity and reproducibility for the preconcentration of Sunset Yellow.

The proposed method was also evaluated by comparing some reported methods for the analysis of Sunset Yellow. It was demonstrated that the LOD value of the present method was comparable to the others, *i.e.*, SPE-HPLC (0.027 μg mL^{-1}) [41], HPLC-UV-DAD (0.05 μg mL^{-1}) [42], HPLC-DAD-ESI-MS (3.5 ng) [43], and LLE-LC-MS (0.01 μg mL^{-1}) [10]. The whole process of extraction, desorption, and detection of Sunset Yellow with the microcolumn containing ANMPC could be accomplished within less than 9 min, demonstrating that the proposed method is a rapid one. Moreover, the present method costs little organic solvent, using less than 0.5 mL methanol for one extraction, indicating that the method is environmentally friendly compared with the HPLC and LLE method. As a result, the developed SPE method for Sunset Yellow has sen-

Table 1. Recovery values (%) for beverage samples (n=3)

Samples	Analyte	Found ($\mu g\ mL^{-1}$)	Recovery mean (%)±SD	
			Level 1	Level 2
Fruit juice 1	Sunset Yellow	<LOD	103.7±2.9	95.3±3.8
Fruit juice 2	Sunset Yellow	5.10±0.05	98.4±1.7	103.6±2.4
Fruit juice 3	Sunset Yellow	<LOD	109.3±1.6	100.1±2.3
Carbonated beverage 1	Sunset Yellow	<LOD	98.0±1.9	104.9±3.7
Carbonated beverage 2	Sunset Yellow	14.75±0.19	97.5±2.7	95.7±3.4
Carbonated beverage 3	Sunset Yellow	9.75±0.57	104.7±4.4	92.8±4.7
Pre-mix cocktail 1	Sunset Yellow	14.38±0.09	100.5±0.9	103.9±0.8
Pre-mix cocktail 2	Sunset Yellow	<LOD	108.6±2.7	104.1±2.8
Pre-mix cocktail 3	Sunset Yellow	4.10±0.06	105.4±1.3	98.1±2.1

sitivity, rapidity, and low consumption of organic solvent.

5. Analysis of Real Samples

To establish the validity of the process, the proposed method was applied in the determination of Sunset Yellow in beverage samples. All the beverage samples are spiked with the Sunset Yellow standard solution at different concentration levels to assess the matrix effects, Level 1 (1 $\mu g\ mL^{-1}$) and Level 2 (2 $\mu g\ mL^{-1}$). Non-spiked samples were also analyzed. As shown in Table 1, the recoveries of Sunset Yellow were obtained in the range of 92.3-109.8% with RSD values of <4.7%. The results indicate that the proposed method is suitable for the determination of Sunset Yellow in beverage samples.

CONCLUSIONS

As-synthesized ANMPC as wadding material was successfully applied to the SPE method for the preconcentration of Sunset Yellow in beverage samples coupled with UV-Vis spectrophotometry. Owing to γ-alumina nanoparticles dispersed in binary porogens (DMSO and dodecanol), ANMPC as the adsorbent exhibited the desirable adsorption ability. Experimental conditions in the processes of preparation of the adsorbent and solid-phase extraction were studied and optimized as follows: synthesis temperature (60 °C), synthesis time (5 h), the dosage of γ-alumina nanoparticles (60 mg), sample flow rate (1.0 mL min^{-1}), sample pH (2.0), eluant concentration (2.0%), and eluant flow rate (0.5 mL min^{-1}). Validation parameters of the proposed method, such as LOD, LOQ, RSDs, and the enrichment factor were satisfactory for the determination of Sunset Yellow. Based on the results, the method for the determination of Sunset Yellow proves itself as a simple, sensitive, and rapid technique.

ACKNOWLEDGEMENTS

The project was supported by College Science Foundation of Taiyuan Institute of Technology in China (No. 2015LQ10) and Innovation and Entrepreneurship Training Program of College Students of Taiyuan Institute of Technology in China (No. GK2015045).

REFERENCES

1. K. S. Minioti, C. F. Sakellariou and N. S. Thomaidis, *Anal. Chim. Acta*, **583**, 103 (2007).
2. K. Golka, S. Kopps and Z. W. Myslak, *Toxicol. Lett.*, **151**, 203 (2004).
3. GB 2760-2011, *Hygiene standards for use of food additives*, Health Ministry of P. R. China, Beijing (2011).
4. W. J. Li, X. Zhou, S. S. Tong and Q. Jia, *Talanta*, **105**, 386 (2013).
5. H.-G. Gao, W.-J. Gong and Y.-G. Zhao, *Anal. Sci.*, **31**, 205 (2015).
6. J. Zhang, M. Wang, S. Chao, W. Wang, Y. He and Z. Chen, *J. Electroanal. Chem.*, **685**, 47 (2012).
7. E. C. Vidotti, J. C. Cancino, C. C. Oliveira and M. C. E. Rollemberg, *Anal. Sci.*, **21**, 149 (2005).
8. N. Djafarzadeh, M. Safarpour and A. Khataee, *Korean J. Chem. Eng.*, **31**, 785 (2014).
9. R. Qi, X. Zhou, X. Li, J. Ma, C. Lu, J. Mu, X. Zhang and Q. Jia, *Analyst*, **139**, 6168 (2014).
10. M. R. Fuh and K. J. Chia, *Talanta*, **56**, 663 (2002).
11. W. Liu, W. J. Zhao, J. B. Chen and M. M. Yang, *Anal. Chim. Acta*, **605**, 41 (2007).
12. Y. Wang, M. Mei, X. Huang and D. Yuan, *Anal. Methods*, **7**, 551 (2015).
13. X. Hu, Q. Cai, Y. Fan, T. Ye, Y. Cao and C. Guo, *J. Chromatogr. A*, **1219**, 39 (2012).
14. X. Yu, Y. Sun, C. Z. Jiang, Y. Gao, Y. P. Wang, H. Q. Zhang and D. Q. Song, *J. Sep. Sci.*, **35**, 3403 (2012).
15. J. Xin, D. Zhao, L. Zhang, Z. Xu, J. Zhou and D. Qu, *Chromatographia*, **73**, 235 (2011).
16. R. Su, X. Zhao, Z. Li, Q. Jia, P. Liu and J. Jia, *Anal. Chim. Acta*, **676**, 103 (2010).
17. K. Naraghi, H. A. Panahi, A. H. Hassani and E. Moniri, *Korean J. Chem. Eng.*, **31**, 1818 (2014).
18. J. Ye, S. Liu, M. Tian, W. Li, B. Hu, W. Zhou and Q. Jia, *Talanta*, **118**, 231 (2014).
19. Q. Geng and W. Cui, *Ind. Eng. Chem. Res.*, **49**, 11321 (2010).
20. K. Mahmoudi, K. Hosni, N. Handi and E. Srasra, *Korean J. Chem. Eng.*, **32**, 274 (2015).
21. Y. Wang and W. Chu, *Ind. Eng. Chem. Res.*, **50**, 8734 (2011).
22. J. Roh, H. N. Umh, C. M. Yoo, S. Rengaraj, B. Lee and Y. Kim, *Korean J. Chem. Eng.*, **29**, 903 (2012).
23. Y. S. Al-Degs, A. H. El-Sheikh, M. A. Al-Ghouti, B. Hemmateenejad and G. M. Walker, *Talanta*, **75**, 904 (2008).
24. Z. Xu, Q. Zhang and H. H. P. Fang, *Crit. Rev. Environ. Sci. Technol.*, **33**, 363 (2003).

25. Y. Guan, Y. Mao, D. Wei, X. Wang and P. Zhu, *Korean J. Chem. Eng.*, **30**, 1810 (2013).
26. J. J. Ye, W. Feng, M. M. Tian, J. L. Zhang, W. H. Zhou and Q. Jia, *Anal. Methods*, **5**, 1046 (2013).
27. B. F. Senkal and E. Yavuz, *Polym. Adv. Technol.*, **17**, 928 (2006).
28. A. Hashem, E. S. Abdel-Halim and H. H. Socker, *Polym. Plast. Tech. Eng.*, **46**, 71 (2007).
29. G. F. Fanta, R. C. Burr, C. R. Russell and C. E. Rist, *J. Appl. Polym. Sci.*, **10**, 929 (1966).
30. M. Wu, R. Wu, Z. Zhang and H. Zou, *Electrophoresis*, **32**, 105 (2011).
31. R. Ahmad and R. Kumar, *Clean: Soil, Air, Water*, **39**, 74 (2011).
32. J. Krenkova and F. Foret, *J. Sep. Sci.*, **34**, 2106 (2011).
33. S. Tong, Q. Liu, Y. Li, W. Zhou, Q. Jia and T. Duan, *J. Chromatogr. A*, **1253**, 22 (2012).
34. J. Kujawa, W. Kujawski, S. Koter, A. Rozicka, S. Cerneaux, M. Persin and A. Larbot, *Colloids Surf., A*, **420**, 64 (2013).
35. F. Meder, T. Daberkow, L. Treccani, M. Wilhelm, M. Schowalter, A. Rosenauer, L. Mäler and K. Rezwan, *Acta Biomater.*, **8**, 1221 (2012).
36. M. Tian, W. Feng, J. Ye and Q. Jia, *Anal. Methods*, **5**, 3984 (2013).
37. Y. J. Chen, R. Z. Jing, S. C. Cheng, Y. H. Wang, Q. J. Wan, L. Y. Xiong and Z. F. He, *J. GuiZhou Agric. Coll.*, **15**, 66 (1996).
38. S. Xie, F. Svec and J. M. J. Frechet, *J. Polym. Sci. Pol. Chem.*, **35**, 1013 (1997).
39. F. Svec and J. M. J. Frechet, *Chem. Mater.*, **7**, 707 (1995).
40. C. H. Shek, J. K. L. Lai, T. S. Gu and G. M. Lin, *Nanostruct. Mater.*, **8**, 605 (1997).
41. N. Yoshioka and K. Ichihashi, *Talanta*, **74**, 1408 (2008).
42. S. P. Alves, D. M. Brum, É. C. Branco de Andrade and A. D. Pereira Netto, *Food Chem.*, **107**, 489 (2008).
43. M. Ma, X. B. Luo, B. Chen, S. P. Sub and S. Z. Yao, *J. Chromatogr. A*, **1103**, 170 (2006).